Letter

Unveiling the graviton mass bounds through the analysis of 2023 pulsar timing array data releases

Sai Wang [1] and Zhi-Chao Zhao [2,*]

[1] *Theoretical Physics Division, Institute of High Energy Physics, Chinese Academy of Sciences, Beijing 100049, the People's Republic of China*
[2] *Department of Applied Physics, College of Science, China Agricultural University, Qinghua East Road, Beijing 100083, the People's Republic of China*

(Received 16 October 2023; accepted 1 March 2024; published 18 March 2024)

Strong evidence for the Helling-Downs correlation curves have been reported by multiple pulsar timing array (PTA) collaborations in the middle of 2023. In this work, we investigate the graviton mass bounds by analyzing the observational data of the overlap reduction functions from the NANOGrav 15-year data release and CPTA first data release. The results from our data analysis display the state-of-the-art upper limits on the graviton mass at 90% confidence level, namely, $m_g \lesssim 8.6 \times 10^{-24}$ eV from NANOGrav and $m_g \lesssim 3.8 \times 10^{-23}$ eV from CPTA. We also study the cosmic-variance limit on the graviton mass bounds, i.e., $\sigma^{\rm CV}_{m_g} = 4.8 \times 10^{-24}\ {\rm eV} \times f/(10\ {\rm year})^{-1}$, with f being a typical frequency band of PTA observations. This is equivalent to the cosmic-variance limit on the speed of gravitational waves, i.e., $\sigma^{\rm CV}_{v_g} = 0.07c$, with c being the speed of light. Moreover, we discuss potential implications of these results for scenarios of ultralight tensor dark matter.

DOI: 10.1103/PhysRevD.109.L061502

Introduction. In Einstein's theory of general relativity, the Hellings-Downs (HD) correlation curves [1] have been shown to characterize the overlap reduction functions (ORFs) due to the existence of a stochastic gravitational-wave background (SGWB) of nano-Hertz band that is detectable for ongoing and future programs of pulsar timing array (PTA). The specific forms of them are solely determined by a null-mass characteristic of gravitational waves. Recently, both the North American Nanohertz Observatory for Gravitational Waves (NANOGrav) [2] and Chinese PTA (CPTA) [3] Collaborations reported strong evidence for a stochastic signal that is spatially correlated among multiple pulsars. In particular, the HD correlation curves were claimed to deserve statistical significance of $\sim 3\sigma - 4\sigma$ by NANOGrav and of 4.6σ by CPTA. Meanwhile, the European PTA (EPTA) [4] and Parkes PTA (PPTA) [5] Collaborations further claimed that their observational results are also compatible with the HD correlation curves.

However, for the massive gravity, the spatial correlations are expected to be different from the standard HD correlation curves. Correspondingly, their theoretical expressions depend on the speed of gravitational waves and hence on the graviton mass, but would recover the results of HD correlation curves in the massless limit [6–9]. The theory of massive gravity was first proposed by Fierz and Pauli in 1939 [10]. Since then, it and its extensions have been comprehensively studied in subsequent decades and multiple upper bounds on the graviton mass have been placed by a large quantity of laboratory and astronomy observations (e.g., see reviews in Ref. [11] and references therein). Meanwhile, these theories of massive gravity have been used for interpreting cosmological phenomena, such as an accelerating expansion rate of the late universe without the need for dark energy [12,13], the observed gravitational effects without the need for additional dark matter [13], and so on. Moreover, constraining the graviton mass with observations from PTA could be helpful to understand the nature of gravity, e.g., its intrinsic symmetry, quantization, etc [14].

During the era of gravitational-wave astronomy, the speed of gravitational waves v_g has been shown by the Advanced LIGO, Virgo and KAGRA (LVK) Collaborations to be compatible with the light speed with a precision $|v_g - 1| \lesssim 10^{-15}$, indicating upper limits on the graviton mass, namely, $m_g \lesssim 10^{-23}$ eV [15,16]. Similar bounds on the graviton mass have also been claimed by other research groups [17,18], who focused on analysis of the NANOGrav 12.5-year PTA data [19]. Moreover, pulsar timing of binary pulsars PSR B1913 + 16 and PSR B1534 + 12 has set an upper limit of $m_g < 7.6 \times 10^{-20}$ eV at 90% confidence level [20]. Forecasting works related to planned space-borne gravitational-wave detectors can be found in Ref. [21].

In this work, we will study the state-of-the-art upper limits on the graviton mass through analysis of the 2023 data releases of NANOGrav and CPTA programs [2,3].

[*] Corresponding author: zhaozc@cau.edu.cn

Though demonstrating strong evidence for the HD correlation curves, these observations have not vetoed other alternative correlations. As shown in Ref. [7], the graviton mass would flatten the spatial correlation curves, since a more-massive graviton has a lower speed. An earlier forecasting work can be found in Ref. [22]. Therefore, we will take into account the specific ORFs for massive gravitons during our practical analysis of the recent PTA datasets from NANOGrav [2] and CPTA [3]. The remaining context of the paper is as follows. In Sec. II, we show the theoretical expressions of ORFs for massive gravitons, with the HD correlation curves being their massless limit. In Sec. III, we show a likelihood method for our data analysis and the resulting bounds on the graviton mass. In Sec. V, we display the concluding remarks and discussion.

Spatial correlation curves for massive gravitons. For simplicity, we consider the helicity-2 modes without loss of generality [23]. In principle, we can study the massive gravity via analyzing its Lagrangian. However, when we focus solely on the propagation of gravitational waves, an equivalent but simple approach seems to concern the dispersion relation of gravitons, i.e.,

$$\omega^2 = k^2 + m_g^2, \tag{1}$$

where m_g denotes the graviton mass, and ω and k stand for the angular frequency and wave number, respectively. The above dispersion relation leads to a definition of the speed of gravitational waves, namely $v_g = d\omega/dk$ [16]. For subluminal gravitons, we can establish a relation between the graviton mass and the speed of gravitational waves, namely,

$$m_g \simeq 1.31 \times 10^{-22}\ \mathrm{eV} \times \frac{f}{\mathrm{year}^{-1}} \times \sqrt{1 - v_g^2}, \tag{2}$$

where $f = \omega/(2\pi)$ is the frequency of gravitational waves, and the light speed is defined as unity, i.e., $c = 1$. For a typical frequency band of gravitational waves, a lower bound on the speed of gravitational waves can be recast into an upper bound on the graviton mass.

Upon the influence of a SGWB, the time of arrivals of radio pulses from two pulsars would be spatially correlated [24–26], with the angular correlation being defined as

$$\gamma_{ab}(v_g, \zeta_{ab}) = \sum_{\ell} \frac{2\ell + 1}{4\pi} C_\ell P_\ell(\cos\zeta_{ab}), \tag{3}$$

where the subscript $_{ab}$ stands for the cross correlation between these two pulsars, as labeled by a and b, with their angular separation ζ_{ab}, and the angular power spectrum C_ℓ is defined as

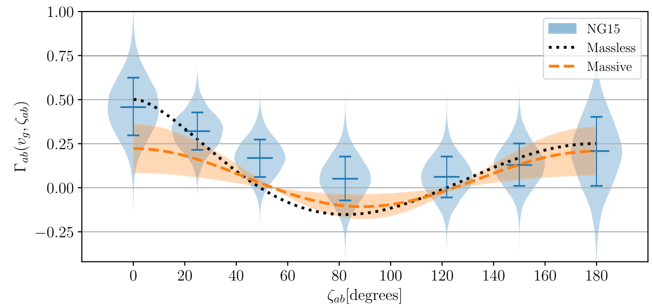

FIG. 1. Comparison between the ORFs of massive gravitons (orange dashed curve denotes $m_g = 7.7 \times 10^{-24}\ \mathrm{eV}^{-1}$) and those of massless gravitons. The orange shaded region stands for 1σ uncertainties due to the cosmic variance. The NANOGrav 15-year data points are also shown as shaded violins for comparison.

$$C_\ell = \frac{1}{\sqrt{\pi}} J_\ell(v_g, fD_a) J_\ell^*(v_g, fD_b), \tag{4}$$

where D_c denotes a distance to the c-th pulsar. To simplify the definition, we have introduced a function of the form

$$J_\ell(v_g, y) = \sqrt{2}\pi i^\ell \sqrt{\frac{(\ell+2)!}{(\ell-2)!}} \int_0^{2\pi y v_g} \frac{dx}{v_g} e^{ix/v_g} \frac{j_\ell(x)}{x^2}, \tag{5}$$

where $j_\ell(x)$ denotes the spherical Bessel function with ℓth multipole. Following Refs. [7,27], we recast the angular correlation $\gamma_{ab}(v_g, \zeta_{ab})$ into the ORFs of massive gravitons, i.e., $\Gamma_{ab}(v_g, \zeta_{ab})$, by normalizing the former such that $\Gamma_{ab}(v_g = 1, \zeta_{ab} = 0^+) = 0.5$, where the subscript $_{ab}$ stands for the correlation of ath and bth pulsars. It is worthy noting that the HD correlation curves would be recovered by the above correlations in the massless limit.

We show the difference between the ORFs of massive gravitons (orange dashed curves) and those of massless gravitons (black dotted curves) in Figs. 1 and 2. We depict these ORFs of massive gravitons by using the best-fit results in the next section. The orange shaded regions stand for the 1σ uncertainties due to the cosmic variance, i.e., $\Delta C_\ell / C_\ell = [2/(2\ell+1)]^{1/2}$. For comparison, we reproduce the observed ORFs by NANOGrav [2] (blue shaded violins in Fig. 1) and CPTA [3] (blue data points with error bars in Fig. 2). It seems that the massive gravitons fit better the observed spatial correlation curves than the massless gravitons. Our data analysis in the subsequent section would be proved to support such a suspicion.[1]

Results from data analysis. In the NANOGrav 15-year data release, there are 67 individual pulsars with timing baselines longer than three years monitored, implying a total of 2,211 distinct pairs, with each pair having a deterministic angular separation. Based on the previous 12.5-year data

[1] Besides our present paper, Ref. [28] supports the same results.

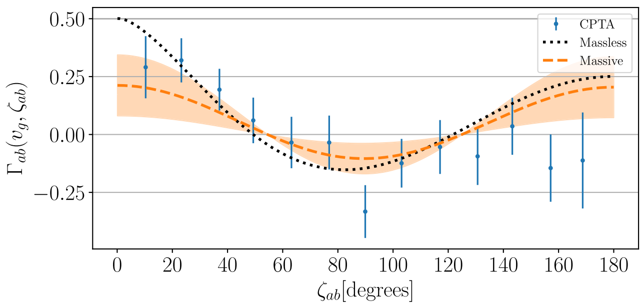

FIG. 2. Comparison between the ORFs of massive gravitons (orange dashed curve denotes $m_g = 3.6 \times 10^{-23}$ eV^{-1}) and those of massless gravitons. The orange shaded region stands for 1σ uncertainties due to the cosmic variance. The CPTA first data release is also shown as data points with error bars for comparison.

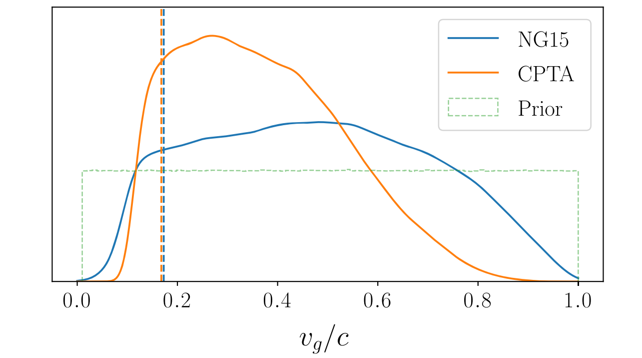

FIG. 3. Posteriors of the speed of gravitational waves v_g inferred from the NANOGrav 15-year data release and the CPTA first data release. The vertical dashed lines stand for the 90% confident lower limits.

release, the authors of Ref. [2] have constructed a minimally modeled Bayesian reconstruction of the inter-pulsar correlation pattern via employing a spline interpolation over seven spline-knot positions, i.e., Fig. 1(d) of the paper. In the CPTA first data release [3], there are 57 individual millisecond pulsars monitored. The 4.6σ statistical significance of the HD correlations between those pulsars has been reported at around 14 nHz, i.e., Fig. 4 of the data-release paper.

Analyzing the above NANOGrav and CPTA observational data of the spatial correlations, we can infer the speed of gravitational waves, or equivalently, the graviton mass, by using the log-likelihood as follows

$$-2 \ln \mathcal{L}(v_g|\mathrm{D}) = \sum_{\zeta_{ab}} \left(\frac{\Gamma_{ab}(v_g, \zeta_{ab}) - \Gamma_{ab}^{\mathrm{D}}}{\sigma_{ab}^{\mathrm{D}}} \right)^2, \qquad (6)$$

where Γ_{ab}^{D} stands for the observed ORFs for the binned angular separation ζ_{ab}, σ_{ab}^{D} stands for the corresponding 1σ uncertainty, D denotes the NANOGrav or CPTA datasets, and the summation runs over all the binned angular separations. It is worthy noting that the above uncertainties σ_{ab}^{D} also contain contributions from the cosmic variance [7,27,29], which contributes to an overall error in the measured inter-pulsar correlation or the harmonic space coefficients, C_l's. That is $(\sigma_{ab}^{\mathrm{D}})^2 = (\sigma_m)^2 + (\sigma_{\mathrm{CV}})^2$, where σ_m denotes the measured error and σ_{CV} arises from the cosmic variance that will also be mentioned in the next section. In other words, we consider the cosmic variance of the correlation in our data analysis, i.e., the orange regions in Figs. 1 and 2.

For our data analysis, the parameter to be inferred is the speed of gravitational waves v_g. We let the corresponding prior probability distribution to be uniform, i.e., $v_g \in [10^{-2}, 1]$, and perform Markov-Chain Monte-Carlo samplings by using the publicly available COBAYA software [30]. We further adopt the publicly available PTAfast package [27] to compute the ORFs of massive gravitons. The resulting posterior probability distribution functions of v_g will be recast into those of m_g, following the relation in Eq. (2). Following the above approach, we will obtain some upper limits on m_g at 90% confidence level and so on.

Our results are shown as follows. Firstly, the posterior probability distributions of v_g are depicted in Fig. 3. We show the results for NANOGrav in a blue curve while those for CPTA in an orange curve. Correspondingly, we label the 90% confident lower limits on v_g with vertical dashed lines with the same coloring. They are shown to be $v_g \gtrsim 0.173$ for NANOGrav and $v_g \gtrsim 0.168$ for CPTA. Based on Fig. 3, it seems that CPTA favors a relatively smaller speed of gravitons, compared with NANOGrav. Secondly, we further display the posterior probability distributions of m_g in Fig. 4. The shaded regions stand for the allowed parameter space at 90% confidence level. To be specific, we display the results for NANOGrav in the blue shaded region and those for CPTA in the orange shaded region. Following Eq. (2), in which f is a frequency corresponding

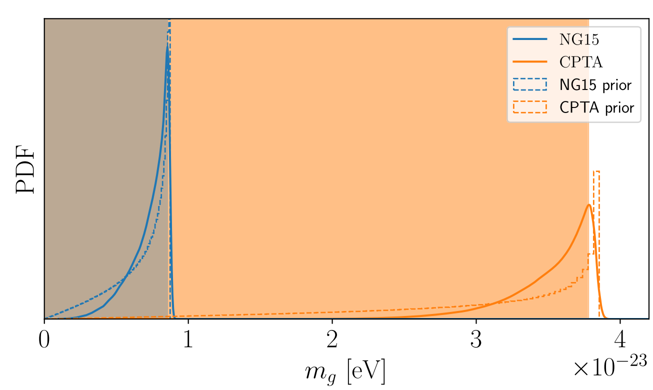

FIG. 4. Posteriors of the graviton mass m_g inferred from the NANOGrav 15-year data release and the CPTA first data release. The shaded regions stand for the allowed parameter space at 90% confidence level.

to the time span of PTA observation, we obtain the upper limits on m_g at 90% confidence level, namely,

$$m_g \lesssim 8.6 \times 10^{-24}\ \mathrm{eV} \tag{7}$$

from NANOGrav and

$$m_g \lesssim 3.8 \times 10^{-23}\ \mathrm{eV} \tag{8}$$

from CPTA. We find that the two bounds are comparable with each other. They stand for the state-of-the-art upper limits on the graviton mass. Moreover, we notice overlapping posteriors for the gravitational wave (GW) speed, while seemingly distant posteriors for the graviton mass. This difference stems from different duty circles or frequency inputs for the NANOGrav and CPTA datasets. In fact, when evaluating Eq. (2), we have used $f = (15\ \mathrm{years})^{-1}$ for the former, while $f = (3.4\ \mathrm{years})^{-1}$ for the latter.

Besides of SGWB with characteristic quadrupolar angular patterns, there are two other common signals with different angular correlations. The first is associated with errors in our clock standards and has a monopolar correlation. The second is due to errors in Solar system ephemerids and has a dipolar correlation. To produce robust upper limits on graviton mass, we also compare the data-derived correlation patterns with a combination of these three correlations. In other words, the latter can be given by

$$\Gamma^{\mathrm{eff}}_{ab}(v_g, \zeta_{ab}) = a + b \times \cos\zeta_{ab} + \Gamma_{ab}(v_g, \zeta_{ab}), \tag{9}$$

where a and b are undetermined parameters. Figure 5 demonstrate comparisons between the posteriors of v_g with and without monopolar and dipolar correlations for NANOGrav and CPTA. However, we find few difference between these results of this joint analysis and those of our present analysis.

In Fig. 4, we find that the posteriors on the graviton mass are not flat. Therefore, it may be more adequate to provide the "measured" values of the model parameters. At 68% C.L., they are given by

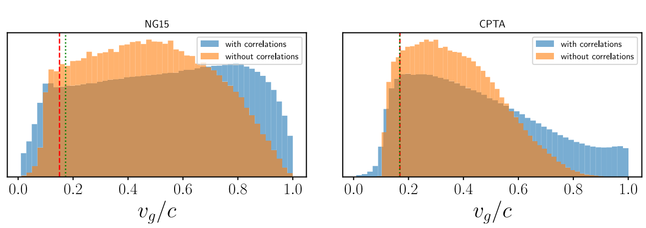

FIG. 5. Comparison between the posteriors with and without monopolar and dipolar correlations inferred from the NG15 (left) and CPTA (right) datasets. The red dashed and green dotted lines represent the 90% C.L. upper limits for the respective cases.

$$m_g = 7.71^{+0.81}_{-1.71} \times 10^{-24}\ \mathrm{eV} \tag{10}$$

for NANOGrav and

$$m_g = 3.61^{+0.17}_{-0.37} \times 10^{-23}\ \mathrm{eV} \tag{11}$$

for CPTA, respectively. The inclination of our results toward the massive graviton hypothesis could arise from several factors that may bias our results. For example, the reported signals may not be solely contributed by a SGWB, but also by unknown physical processes, e.g., the aforementioned scalar or vector correlations. On the other hand, there may also be unknown systematics within the datasets, which should be checked by future observations. However, we cannot exclude the possibility that the speed of gravitational waves is indeed subluminal. It can also be vetoed or confirmed by future observations.

Cosmic-variance limit on the graviton mass bounds. Our study can be further improved by upcoming PTA observations. At present, the detection of pulsars is on the rise, with an increasing number of newly constructed telescopes offering heightened sensitivity and producing data of continually improving quality. Concurrently, advancements in pulsar modeling techniques and data processing tools are allowing for more effective noise suppression. Moreover, the accumulation of data over extended periods is facilitating an increase in signal-to-noise ratio and enabling observations across diverse frequency bands. This has resulted in the acquisition of increasingly powerful tools for PTA observations.

However, the cosmic variance, i.e., $\Delta C_\ell / C_\ell = [2/(2\ell+1)]^{1/2}$, would inevitably introduce an uncertainty to inferences of the graviton mass.[2] For example, it can bring about uncertainties on $\Gamma_{ab}(v_g, \zeta_{ab})$, as shown as the orange shaded regions in Figs. 1 and 2, which could be recast into uncertainties on m_g, as studied in this section. Due to the cosmic variance, we inquire the maximal capability of PTA in constraining the graviton mass and whether it is sufficient to challenge theories of gravity beyond general relativity. We study this issue in the following.

[2]It is challenging to discuss details of the cosmic variance in this short paper. Here, we provide only a brief review of the concept of cosmic variance. Traditionally, it is popular to consider the cosmic variance in cosmological data analysis, e.g., temperature and polarization anisotropies in the cosmic microwave background (CMB) [31], etc. Recently, a similar proposal was originally introduced to the community of PTA in Refs. [29,32]. Subsequently, the cosmic variance was further considered in PTA-relevant studies of additional polarization modes of gravitational waves in Ref. [27]. We strongly recommend readers to refer to these papers if they wish to find more details of the cosmic variance.

To investigate the cosmic-variance limit, we consider an ideal PTA observation, which does not have instrumental uncertainties. In other words, we assume that all the uncertainties arise from the cosmic variance. As a first step, we should get the cosmic-variance limit on the speed of gravitational waves. For simplicity, we follow an approach of Fisher matrix, i.e.,

$$F = \int d\zeta_{ab} \left(\frac{1}{\sigma_{ab}}\right)^2 \left(\frac{\partial\Gamma_{ab}(v_g, \zeta_{ab})}{\partial v_g}\right)^2 \qquad (12)$$

where σ_{ab} stands for the 1σ uncertainty on Γ_{ab} arising from the cosmic variance. Here, we consider a fiducial model with massless gravitons, indicating $v_g = 1$ during derivations of the Fisher matrix. By evaluating F^{-1}, we obtain the cosmic-variance limit on the speed of gravitational waves, i.e., $\sigma_{v_g}^{\mathrm{CV}} = 0.07$. By using Eq. (2), we recast it into the cosmic-variance limit on the graviton mass bounds, namely,

$$\sigma_{m_g}^{\mathrm{CV}} = 4.8 \times 10^{-24}\ \mathrm{eV} \times \frac{f}{(10\ \mathrm{year})^{-1}}, \qquad (13)$$

where f typically denotes the lowest frequency band of PTA observations, which can roughly correspond to the observational time span. This inevitable uncertainty cannot be gotten rid of by any PTA, indicating that it is intrinsic. In other words, it stands for the maximal capability of PTA in measuring the graviton mass.

Conclusions and discussion. In this work, we investigated the graviton mass bounds through analysis of the NANOGrav 15-year dataset and the CPTA first data release. By analyzing the data points of ORFs from these two observatories, we inferred the allowed parameter intervals for the speed of gravitational waves, particularly, its posterior probability distributions. By further recasting them into the posterior probability distributions of graviton mass, we obtained the state-of-the-art upper limit on the graviton mass, namely, $m_g \lesssim 8.6 \times 10^{-24}$ eV at 90% confidence level.

We found that these new bounds on the graviton mass are comparable to the most recent one reported by the LVK Collaborations, i.e., $m_g < 1.27 \times 10^{-23}$ eV at 90% confidence level [16]. However, our study is solely based on the form of ORFs. Therefore, our work has two obvious advantages, compared with those works relevant to LVK. The first one is independence on gravitational-wave sources. The second one is no requirement of prior knowledge of the waveforms. In addition, the findings observed by PTA could effectively supplement those recorded by LVK, since they could compose a multiband study of the graviton mass.

Furthermore, we investigated the cosmic-variance limit on the graviton mass bounds from any PTA observations of SGWB, following an approach analogue to the study of CMB. We found this inevitable cosmic-variance limit to be $\sigma_{m_g}^{\mathrm{CV}} = 4.8 \times 10^{-24}\ \mathrm{eV} \times f/(10\ \mathrm{year})^{-1}$, with f being the typical frequency band of PTA observations of SGWB. As an intrinsic uncertainty, it restricts the maximal capability of PTA in measuring the graviton mass. Moreover, we also obtained the cosmic-variance limit on the speed of gravitational waves, i.e., $\sigma_{v_g}^{\mathrm{CV}} = 0.07$.

One may wonder why the results on the NANOGrav data does not look consistent with those of a subsequent work [33], which adopts the same data to constrain the GW speed. There might be several potential reasons to account for this discrepancy. A notable reason is the inclusion of cosmic variance in our analysis, a factor that was not accounted for in that work. The other reason involves an inherent difference between our model and that of Ref. [33], leading to, e.g., different priors for the two works.

There might be implications of our study for scenarios of ultralight tensor dark matter [34,35], which could account for the mystery of dark matter in the universe. In particular, the ultralight dark matter in the mass range $m_{\mathrm{uldm}} \sim 10^{-22}$ eV was used for conquering several shortcomings of the traditional cold dark matter [36,37]. To some extent, the ultralight dark matter behaves like the massive gravitons, indicating possible imprints of it on PTA observations [38–40]. Since our results have been obtained through analysis of the recent PTA datasets, we can infer that the preferred mass range of ultralight tensor dark matter is also compatible with the upper bounds on graviton mass shown by our current work. A related work resulting from detailed analysis of the NANOGrav 12.5-year dataset can be found in Ref. [41].

Acknowledgments. We acknowledge Dr. R. C. Bernardo for helpful discussion. S. W. is partially supported by the National Natural Science Foundation of China (Grant No. 12175243), the National Key R&D Program of China No. 2023YFC2206403, the Science Research Grants from the China Manned Space Project with No. CMS-CSST-2021-B01, and the Key Research Program of the Chinese Academy of Sciences (Grant No. XDPB15). Z. C. Z. is supported by the National Key Research and Development Program of China Grant No. 2021YFC2203001. This work is supported by the High-performance Computing Platform of China Agricultural University.

[1] R.W. Hellings and G.S. Downs, Upper limits on the isotropic gravitational radiation background from pulsar timing analysis., Astrophys. J. Lett. **265**, L39 (1983).

[2] NANOGrav Collaboration, The NANOGrav 15-year data set: Evidence for a gravitational-wave background, Astrophys. J. Lett. **951**, L8 (2023).

[3] H. Xu *et al.*, Searching for the nano-hertz stochastic gravitational wave background with the Chinese pulsar timing array data release I, Res. Astron. Astrophys. **23**, 075024 (2023).

[4] J. Antoniadis *et al.*, The second data release from the European pulsar timing array III. Search for gravitational wave signals, Astron. Astrophys. **678**, A50 (2023).

[5] D. J. Reardon *et al.*, Search for an isotropic gravitational-wave background with the Parkes pulsar timing array, Astrophys. J. Lett. **951**, L6 (2023).

[6] Q. Liang and M. Trodden, Detecting the stochastic gravitational wave background from massive gravity with pulsar timing arrays, Phys. Rev. D **104**, 084052 (2021).

[7] R. C. Bernardo and K.-W. Ng, Stochastic gravitational wave background phenomenology in a pulsar timing array, Phys. Rev. D **107**, 044007 (2023).

[8] R. C. Bernardo and K.-W. Ng, Testing gravity with cosmic variance-limited pulsar timing array correlations, arXiv:2306.13593.

[9] R. C. Bernardo and K.-W. Ng, Hunting the stochastic gravitational wave background in pulsar timing array cross correlations through theoretical uncertainty, J. Cosmol. Astropart. Phys. 08 (2023) 028.

[10] M. Fierz and W. Pauli, On relativistic wave equations for particles of arbitrary spin in an electromagnetic field, Proc. R. Soc. A **173**, 211 (1939).

[11] C. de Rham, J. T. Deskins, A. J. Tolley, and S.-Y. Zhou, Graviton mass bounds, Rev. Mod. Phys. **89**, 025004 (2017).

[12] T. Kahniashvili, A. Kar, G. Lavrelashvili, N. Agarwal, L. Heisenberg, and A. Kosowsky, Cosmic expansion in extended quasidilaton massive gravity, Phys. Rev. D **91**, 041301 (2015).

[13] S. L. Dubovsky, P. G. Tinyakov, and I. I. Tkachev, Massive graviton as a testable cold dark matter candidate, Phys. Rev. Lett. **94**, 181102 (2005).

[14] G. Janssen *et al.*, Gravitational wave astronomy with the SKA, Proc. Sci. AASKA14 (**2015**) 037 [arXiv:1501.00127].

[15] LIGO Scientific and Virgo Collaborations, Tests of general relativity with the binary black hole signals from the LIGO-Virgo catalog GWTC-1, Phys. Rev. D **100**, 104036 (2019).

[16] LIGO Scientific, VIRGO, and KAGRA Collaborations, Tests of general relativity with GWTC-3, arXiv:2112.06861.

[17] Y.-M. Wu, Z.-C. Chen, and Q.-G. Huang, Search for stochastic gravitational-wave background from massive gravity in the NANOGrav 12.5-year dataset, Phys. Rev. D **107**, 042003 (2023).

[18] R. C. Bernardo and K.-W. Ng, Constraining gravitational wave propagation using pulsar timing array correlations, Phys. Rev. D **107**, L101502 (2023).

[19] NANOGrav Collaboration, The NANOGrav 12.5 yr data set: Search for an isotropic stochastic gravitational-wave background, Astrophys. J. Lett. **905**, L34 (2020).

[20] L. S. Finn and P. J. Sutton, Bounding the mass of the graviton using binary pulsar observations, Phys. Rev. D **65**, 044022 (2002).

[21] Q. Gao, Constraint on the mass of graviton with gravitational waves, Sci. China Phys. Mech. Astron. **66**, 220411 (2023).

[22] K. Lee, F. A. Jenet, R. H. Price, N. Wex, and M. Kramer, Detecting massive gravitons using pulsar timing arrays, Astrophys. J. **722**, 1589 (2010).

[23] C. de Rham, Massive gravity, Living Rev. Relativity **17**, 7 (2014).

[24] K.-W. Ng, Redshift-space fluctuations in stochastic gravitational wave background, Phys. Rev. D **106**, 043505 (2022).

[25] C. M. F. Mingarelli and T. Sidery, Effect of small interpulsar distances in stochastic gravitational wave background searches with pulsar timing arrays, Phys. Rev. D **90**, 062011 (2014).

[26] C. M. F. Mingarelli, T. Sidery, I. Mandel, and A. Vecchio, Characterizing gravitational wave stochastic background anisotropy with pulsar timing arrays, Phys. Rev. D **88**, 062005 (2013).

[27] R. C. Bernardo and K.-W. Ng, Pulsar and cosmic variances of pulsar timing-array correlation measurements of the stochastic gravitational wave background, J. Cosmol. Astropart. Phys. 11 (2022) 046.

[28] R. C. Bernardo and K.-W. Ng, Beyond the Hellings-Downs curve: Non-Einsteinian gravitational waves in pulsar timing array correlations, arXiv:2310.07537.

[29] B. Allen, Variance of the Hellings-Downs correlation, Phys. Rev. D **107**, 043018 (2023).

[30] J. Torrado and A. Lewis, COBAYA: Code for Bayesian analysis of hierarchical physical models, J. Cosmol. Astropart. Phys. 05 (2021) 057.

[31] Planck Collaboration, Planck 2018 results. VI. Cosmological parameters, Astron. Astrophys. **641**, A6 (2020).

[32] B. Allen and J. D. Romano, Hellings and Downs correlation of an arbitrary set of pulsars, Phys. Rev. D **108**, 043026 (2023).

[33] Y.-C. Bi, Y.-M. Wu, Z.-C. Chen, and Q.-G. Huang, Constraints on the velocity of gravitational waves from NANOGrav 15-year data set, arXiv:2310.08366.

[34] L. Marzola, M. Raidal, and F. R. Urban, Oscillating spin-2 dark matter, Phys. Rev. D **97**, 024010 (2018).

[35] S. F. Hassan and R. A. Rosen, Bimetric gravity from ghost-free massive gravity, J. High Energy Phys. 02 (2012) 126.

[36] W. Hu, R. Barkana, and A. Gruzinov, Cold and fuzzy dark matter, Phys. Rev. Lett. **85**, 1158 (2000).

[37] L. Hui, J. P. Ostriker, S. Tremaine, and E. Witten, Ultralight scalars as cosmological dark matter, Phys. Rev. D **95**, 043541 (2017).

[38] T. Broadhurst, C. Chen, T. Liu, and K.-F. Zheng, Binary supermassive black holes orbiting dark matter solitons: From the dual AGN in UGC4211 to nanoHertz gravitational waves, arXiv:2306.17821.

[39] R. A. Konoplya and A. Zhidenko, Asymptotic tails of massive gravitons in light of pulsar timing array observations, arXiv:2307.01110.

[40] J. Yang, N. Xie, and F. P. Huang, Nano-Hertz stochastic gravitational wave background as hints of ultralight axion particles, arXiv:2306.17113.

[41] Y.-M. Wu, Z.-C. Chen, and Q.-G. Huang, Pulsar timing residual induced by ultralight tensor dark matter, J. Cosmol. Astropart. Phys. 09 (2023) 021.